INTERACTION OF AN EXPLOSIVELY DRIVEN CRACK WITH A LARGE FLAW

A. Shukla

Department of Mechanical Engineering and Applied Mechanics, University of Rhode Island, Kingston, Rhode Island 02881, USA

ABSTRACT

Dynamic photoelasticity together with high speed photography is utilized to study the interaction of an explosively driven crack with a large flaw in unloaded and compressively loaded models. Experimental data obtained are analysed to study flaw-wave interaction and flaw-crack interaction. The results indicate a strong influence of the stress field surrounding the running crack on the stationary flow. The flaw tip closer to the running crack initiates in unloaded models even before the running crack terminates into the flaw. Initial compression tends to delay secondary crack initiation.

KEYWORDS

Dynamic photoelasticity, isochromatic fringes, stress intensity factor, mixed mode stress field, stress waves.

INTRODUCTION

Explosive crack propagation in a fractured media is of special interest to rock mechanics community. Examination of core samples taken from Devonian Shale indicate that it is a fractured media whose gas producing capabilities may be highly dependent upon the characteristics of its fracture system. Moreover, it is felt that this fracture system could greatly affect the propagation of a pressurized crack from a borehole during stimulation.

When explosion occurs in a prenotched borehole a complicated system of elastic stress waves followed by a crack network are generated. The waves travel faster than the crack and interact with the flaws which are already existing in the material. While this interaction is going on cracks generated at the borehole and traveling with high velocity and stress intensity factor come and hit the flaws which might still be stationary or have started to move during the flaw-wave interaction. The first phenomenon of flaw-wave interaction itself is important and has received considerable attention in recent years. A theoretical study by Chen and Sih [1] and experimental studies by Smith [2] and Rossmanith and Shukla [3] discuss flaw-wave interaction in

terms of wave diffraction and mixed mode stress field generated at the flaw tip. However, experimental and analytical research in dynamic flaw-crack interaction is rather limited.

This study focuses attention on the dynamic interaction between an explosively generated crack and a stationary central flaw in a sheet of a brittle polyester material Homalite 100. This material has been chosen as it behaves like rock [4] at high strain rates of loading. Photoelastic fringe patterns obtained by high speed photography during flaw-wave interaction and flaw-crack interaction are analysed and discussed. The secondary crack initiation and propagation from the stationary flaw is shown.

EXPERIMENTAL PROCEDURE

The geometry of the specimens used is shown in Fig. 1. The specimens were 9" long and 6" wide and were fabricated from 0.5" thick sheets of Homalite 100. The properties of this material have been characterized by Dally and Kobayashi [5]. The specimens had a 1.5" diameter borehole which was notched to a length of 1/4" so as to direct the explosively generated crack to the center of a premachined flaw. This flaw was 1.5" long and 0.008" wide and was located 3" from the center of the borehole. In the experiments the borehole was charged with 125 mg of PETN. The pressure containment device consisted of two circular steel caps held by a hollow perforated bolt within which the explosive charge was detonated. This device has the effect of somewhat cushioning the explosion and retaining the pressure in the borehole for a comparatively long time after detonation.

The models were placed in the optical bench of a high speed Cranz Schardin type camera. The optical bench of this camera is shown in Fig. 2.

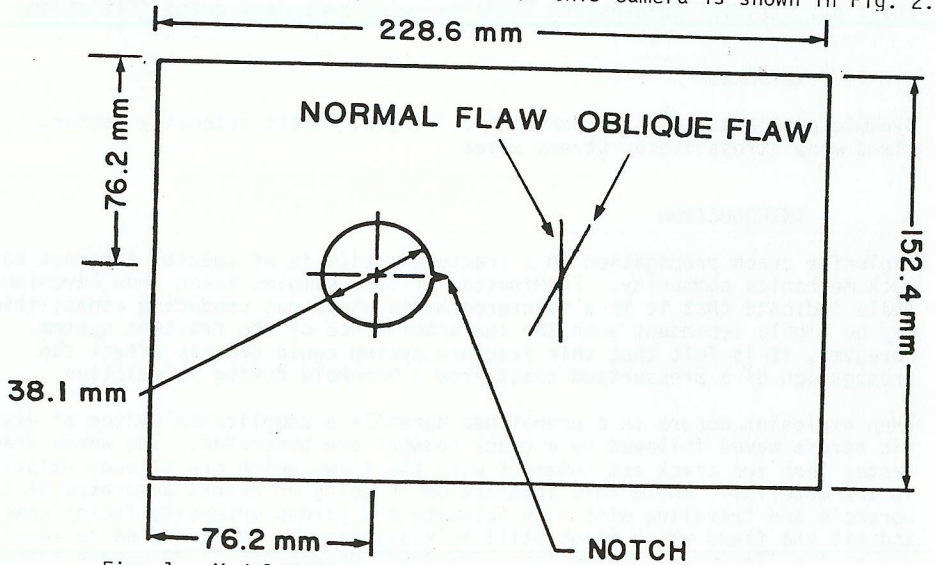

Fig. 1. Model Geometry Representing a Large Flaw in a Monolithic Specimen

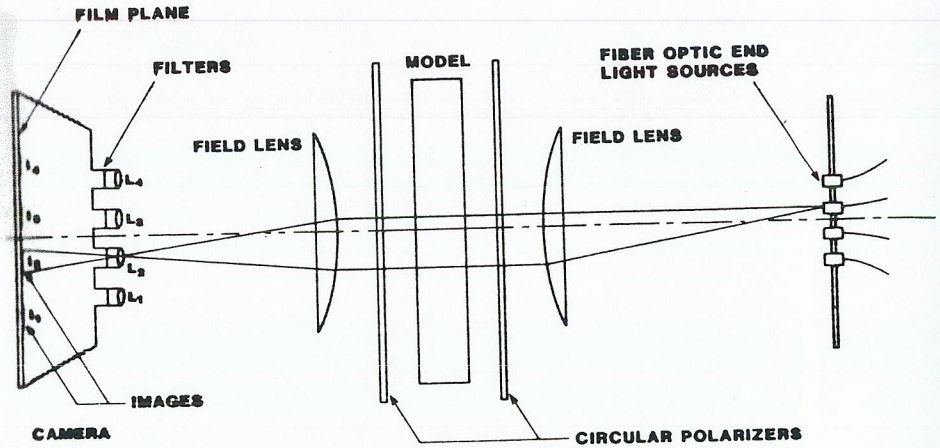

Fig. 2. Optical Bench of the High Speed Camera

The spark gaps are initially charged to 15 KV dc and then discharged upon receiving a trigger signal in a time controlled sequence. The discharging produces a potential difference on two sides of the spark gap causing the spark to jump and producing an intense source of light. The light from each spark is collected with a field lens, circularly polarized and passed through the model. Light coming out from the model is repolarized and then focussed on a set of camera lenses. With this arrangement each image of the dynamic event can be recorded at a different location on a sheet of stationary film. In these experiments the camera was operated at a low framing rate to provide a sequence of sixteen frames for an observation period of 400-500 μs. The time of camera triggering after detonation was controlled with a time delay generator.

A series of three experiments were performed in which the flaw geometry and the preload on the specimen were varied. The results from these experiments are discussed in the following section.

RESULTS AND DISCUSSION

In the first experiment the flaw was machined so that the running crack would hit it at normal incidence. A typical set of isochromatic fringes obtained during the experiment are shown in Fig. 3. Isochromatic fringes are lines of constant maximum shear stress. Frame 1 at 52.5 μs shows the P wave interaction with the flaw tip. As the wave hits the flaw tips it is diffracted and scattered. The resulting stress field $\sigma_{ij}(x,y,t)$ generated about the crack tip is composed of the incident wave $\sigma_{ij}^{i}(x,y,t)$ and the diffracted P and SV waves of $\sigma_{ij}^{s}(x,y,t)$:

$$\sigma_{ij}(x,y,t) = \sigma_{ij}^{i}(x,y,t) + \sigma_{ij}^{s}(x,y,t)$$

where the scattered field must satisfy the condition

$$\sigma_{ij}^{s} \to 0 \text{ as } \sqrt{x^2 + y^2} \to \infty$$

If the crack occupies a line L along y = 0, the normal and shear stress on L are required to vanish such that the boundary conditions are satisfied:

$$\sigma_{yy}{}^{i}(x,o,t) + \sigma_{yy}{}^{s}(x,o,t) = 0, \quad x \varepsilon L$$

$$\sigma_{xy}{}^{i}(x,o,t) + \sigma_{xy}{}^{s}(x,o,t) = 0, \quad x \varepsilon L$$

The mixed mode problem has been solved theoretically [1] where for convenience the fracture problem is divided into a symmetric part [Mode 1] and an anti symmetric part [Mode 2]. The corresponding mixed boundary conditions are:

Mode 1:

$$V_y{}^{s}(x,o,t) = \sigma_{xy}{}^{s}(x,o,t) = 0, \quad x \notin L$$

$$\sigma_{yy}{}^{s}(x,o,t) = -\sigma_{yy}{}^{i}(x,o,t);$$

$$\sigma_{xy}{}^{s}(x,o,t) = 0, \quad x \varepsilon L$$

Mode 2:

$$U_x^{s}(x,o,t) = \sigma_{yy}{}^{s}(x,o,t) = 0, \quad x \notin L$$

$$\sigma_{xy}{}^{s}(x,o,t) = -\sigma_{xy}{}^{i}(x,o,t);$$

$$\sigma_{yy}{}^{s}(x,o,t) = 0, \quad x \varepsilon L$$

The solution of the original problem is obtained by superposition of the particular pure mode solutions. In this paper the stress field is evaluated from experimental data using the properties of isochromatic fringes.

In frame 1 at t = 52.5 μs the leading compressive part of the P-wave hits the flaw tip. Both the tips of the flaw show typical mixed mode isochromatic fringes. These fringes are evaluated using multipoint method of Sanford and Dally [5] and give a K_I value of = 0.55 MPa$\sqrt{m}$ and K_{II} value of 0.1 MPa$\sqrt{m}$ and stress field parallel to the crack σ_{ox} = 1.88 MPa. As the wave passes over the flaw the stress field at the tips oscillates but never is large enough to initiate the flaw. In the mean time the prenotch at the borehole is initiated because of the pressure in the borehole. This crack travels at a high constant velocity of 380 m/s towards the center of the flaw as shown in Fig. 4. The stress field from this crack tip begins to interact with the flaw at about 133.5 μs as shown in frame 2 of Fig. 3. The interaction is stronger with the flaw tip A as the crack is closer to it. The strong tensile field associated with the running crack initiates tip A at about 140 μs as shown in Fig. 4. This tip initiates at an angle of 130° to the flaw at a constant velocity of 340 m/s. Tip B does not initiate until the crack has terminated at the flaw. Frame 3 of Fig. 3 shows the initiation of tip B. The outward movement of the borehole crack walls produces shearing force at tip B. This is reflected in fringe pattern which has a high mode 2 component. The initiation time of this tip is again obtained from Fig. 4 and is about 173 μs which is about 10 μs after the crack terminated at the flaw. Both tips after initiation travel with constant velocity parallel to each other till they break the model.

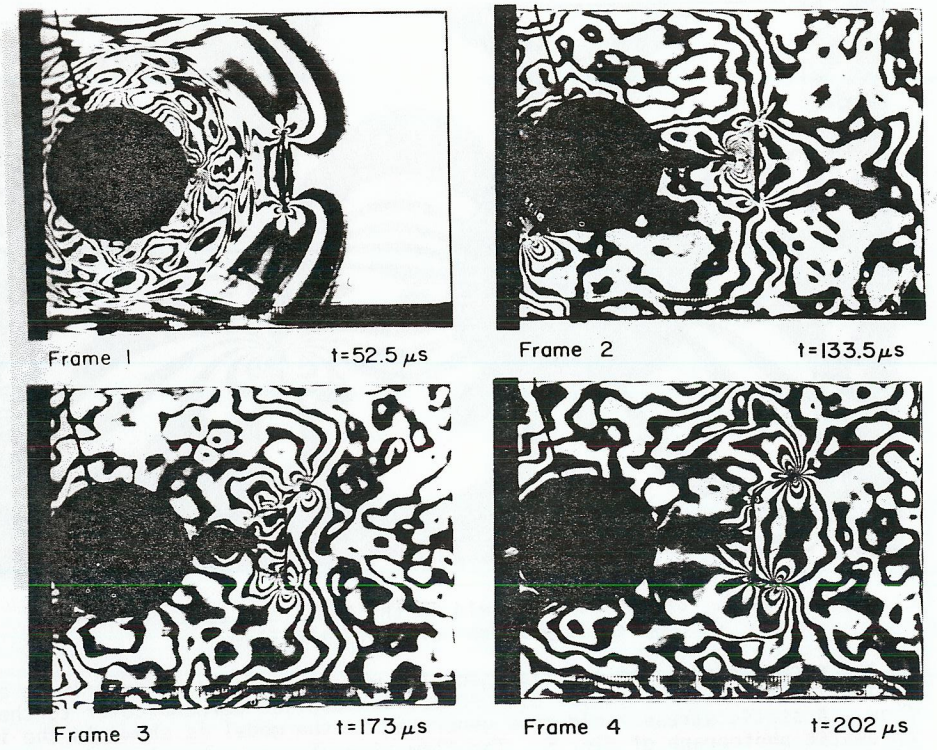

Fig. 3. Dynamic Isochromatics showing Crack Behavior when Intersecting a Premachined Flaw at Normal Incidence

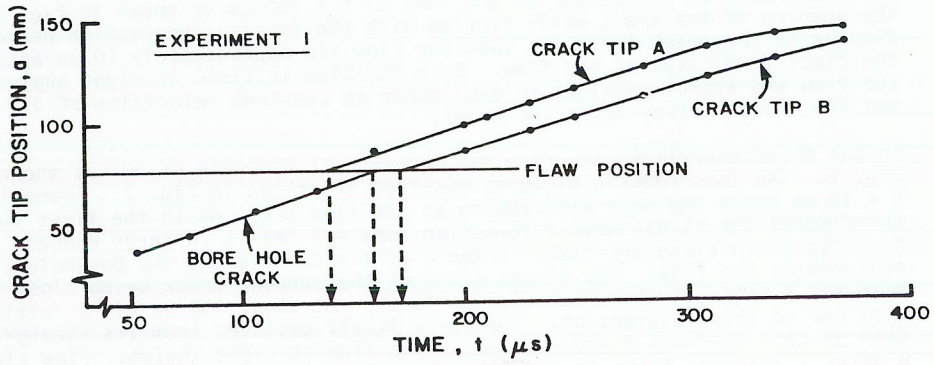

Fig. 4. Crack Tip Position as a Function of Time

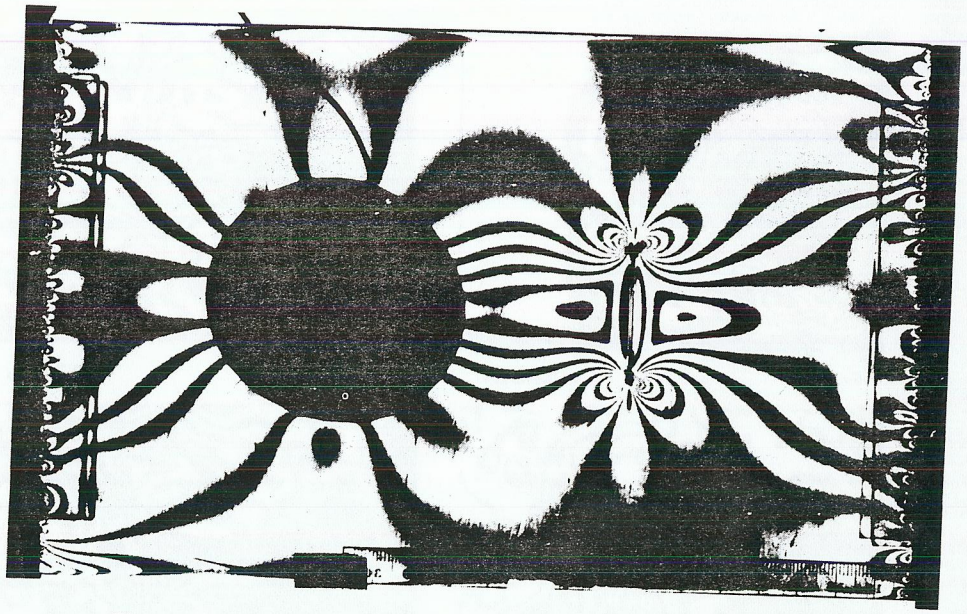

Fig. 5. Static Stress Field in the Model Due to a Compressive Stress Normal to the Flaw

In the second experiment the flaw geometry was the same as in experiment one. An initial compressive stress of 1070 psi was applied perpendicular to the flaw. A static stress field thus generated in the model is shown in the isochromatic photograph of Fig. 5. The flaw tips show a high value of stress intensity factor K_I = 1.96 MPa$\sqrt{m}$ which matches well with the standard central crack equation [6]. Figure 6 shows the interaction of the waves and the crack with the flaw. As the stress wave passes over the flaw the mixed mode stress field changes with time but the flaw does not initiate. The crack initiated at the borehole travels with a constant velocity of 380 m/s and terminates at the center of the flaw at t = 160 μs as shown in Fig. 7. The opening of the crack walls coupled with the initial compression perpendicular to the crack initiates both the flaw tip approximately 10 μs after the crack terminates at the flaw. Both the tips initiate at right angles to the flaw and travel parallel to each other at constant velocities of 370 m/s and 340 m/s till they break the model.

In the third experiment the flaw was machined at an angle of 30° as shown in Fig. 1. The isochromatic pictures obtained are shown in Fig. 7. Frame 1 at t = 40 μs shows the wave diffraction at the flaw tip. As in the first two experiments the stress wave interaction does not result in large enough stresses to initiate the flaw. Frame 2 at t = 97 μs shows the borehole crack approaching the flaw. The stress field of the running crack being close to flaw tip B begins to interact with it first. At about 100 μs tip B initiates due to this interaction. The crack itself deviates from its straight path as seen in frame 3 and approaches the flaw at right angles. Flaw tip B after initiation turns towards the borehole, curves and terminates at the wall of the borehole crack also at right angles at about 180 μs. Flaw tip A initiates after the crack has terminated at the flaw possibly due to the

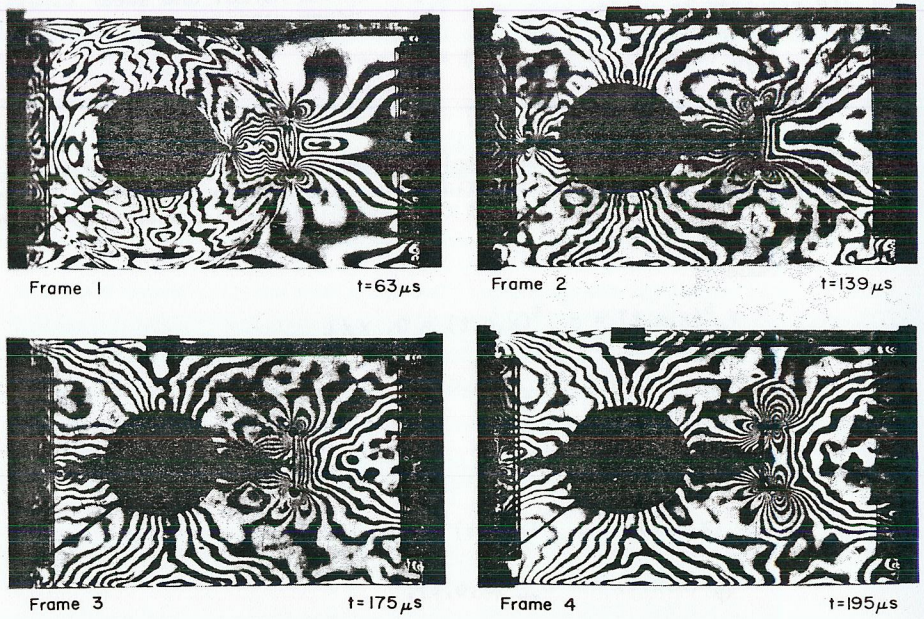

Fig. 6. Dynamic Isochromatics Showing Crack Behavior when Intersecting a Premachined Flaw Subjected Initially to Compressive Stresses

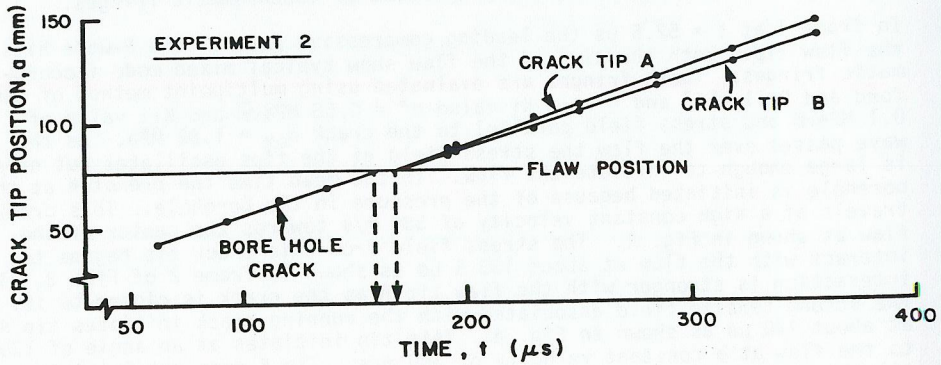

Fig. 7. Crack Tip Position as a Function of Time

Fig. 8. Dynamic Isochromatics Showing Crack Behavior when Intersecting a Premachined Flaw at an Oblique Angle

opening of the crack wall. It travels in opposite direction to the tip B in a zig-zag path across the specimen.

CONCLUSION

Dynamic photoelasticity was employed to provde 'whole field' data to study interaction of explosively generated waves and crack with a large flaw in an unloaded and a compressively loaded photoelastic model. The data obtained showed that:

1. In all three experiments the stress intensification at the flaw tips due to stress wave interaction was not large enough to produce initiation.
2. The running crack tip stress field did produce initiation of the flaw tips closer to it in unloaded specimens even before the crack terminated at the flaw.
3. The flaw tips away from the crack initiated after the crack had terminated at the flaw possibly due to additional loading created by the crack wall movement.
4. In all these experiments both the flaw tips initiated during the experiment.
5. Initial compression tends to delay secondary crack initiation and also influences the propagation direction after initiation.

The author wishes to emphasize the qualitative rather than the quantitative nature of the results. At present data reduction methods for the determination of stress intensity factors associated with transient and gradient stress fields are not completely developed. However, the results obtained do give us an insight into crack-wave and crack-crack interaction problems.

ACKNOWLEDGEMENT

The author acknowledges the support of DOE under grant No. DE-AC21-79MC12010 and NSF under grant No. MEA-8203277. Thanks are also due to Dr. W.L. Fourney for his encouragement and support.

REFERENCES

1. Chen, P.E., and Sih, G.C. (1977). Chap. 1 and 3 of Elastodynamic Crack Problems, Mechanics of Fracture 4, edited by G.C. Sih, Noordhoff International Publication, Leyden.
2. Smith, D.G. (1971). A photoelastic investigation of stress wave loading of a crack. SESA Spring Meeting, Salt Lake City, Utah.
3. Rossmanith, H.P., and Shukla, A. (1981). Experimental Mechanics, Vol. 21, No. 11, pp. 415-422.
4. Fourney, W.L., and Barker, D.B. (1979). Effect of time delay on fragmentation in a jointed model, University of Maryland Report submitted to NSF.
5. Kobayashi, T., and Dally, J.W. (1977). ASTM STP 672, Fast Fracture and Crack Arrest.
6. Tada, H., Paris, P.C., and Irwin, G.R. The Stress Analysis of Cracks Handbook.